Separation and Purification Technology 233 (2020) 115961

Contents lists available at ScienceDirect

Separation and Purification Technology

journal homepage: www.elsevier.com/locate/seppur

Heterogeneous catalyst ozonation of Direct Black 22 from aqueous solution in the presence of metal slags originating from industrial solid wastes

N.T. Hien (PhD)[a,b], Lan Huong Nguyen (PhD)[c], Huu Tap Van (PhD)[d,*], Thi Dong Nguyen[d], Thi Hong Vien Nguyen[d], Thi Hong Huyen Chu[d], Tien Vinh Nguyen (PhD)[e], Van Tuyen Trinh (Prof.)[f], Xuan Hoa Vu (PhD)[g], Kosar Hikmat Hama Aziz (PhD)[h]

[a] Ceramics and Biomaterials Research Group, Advanced Institute of Materials Science, Ton Duc Thang University, Ho Chi Minh City, Vietnam
[b] Faculty of Applied Sciences, Ton Duc Thang University, Ho Chi Minh City, Vietnam
[c] Faculty of Environment – Natural Resources and Climate Change, Ho Chi Minh City University of Food Industry (HUFI), 140 Le Trong Tan Street, Tay Thanh Ward, Tan Phu District, Ho Chi Minh City, Vietnam
[d] Faculty of Natural Resources and Environment, Thai Nguyen University of Sciences (TNUS), Tan Thinh Ward, Thai Nguyen City, Vietnam
[e] Faculty of Engineering and IT, University of Technology Sydney (UTS), Box 123, Broadway, Sydney, PO, Australia
[f] Institute of Environmental Technology – Vietnam Academy of Science and Technology, No 18, Hoang Quoc Viet road, Ha Noi City, Vietnam
[g] Institute of Research and Development, Duy Tan University, Da Nang 550000, Vietnam
[h] Department of Chemistry, College of Science, University of Sulaimani, Kurdistan Region, Qlyasan Street, Sulaimani City 46001, Iraq

ARTICLE INFO

Keywords:
Direct Black 22 (DB22)
Zinc slag (Zn-S)
Heterogeneous catalyst
Ozonation processes

ABSTRACT

This study developed a low cost catalyst, namely, zinc slag (Zn-S) for the ozonation process of Direct Black 22 (DB22) from aqueous solutions. Among five different kind of low cost metal slags including Fe-S, Cu-S, Cd-S, Pb-S and Zn-S, the Zn-S slag was selected as an efficient catalyst in this study. Zn-S contained mainly zinc (Zn) and calcium (Ca) discharged from zinc slag waste in Vietnam. It was found that Zn-S could effectively decolonize and mineralize DB22 through heterogeneous catalytic ozonation. The degradation kinetic of DB22 followed the pseudo-first order model. The best removal efficiency of DB22 ($Zn\text{-}S/O_3/H_2O_2$ (76%) > $Zn\text{-}S/O_3$ (69%) > O_3/H_2O_2 (66%) > O_3 (55% for COD) occurred at pH 11 for heterogeneous catalytic ozonation processes with Zn-S as the catalyst as well as ozone alone and perozone processes due to fast decomposition of O_3 in alkaline solution to generate powerful and non-selective OH radicals. An increase in decolonization and mineralization rate was observed when increasing the Zn-S dosage from 0.125 g/L to 0.75 g/L for $Zn\text{-}S/O_3$ and 0.125 g/L to 1.0 g/L for $Zn\text{-}S/O_3/H_2O_2$. The K values of the pseudo-first order model followed the same sequence as mineralization rates of DB22 in term of COD removal. Ca and Zn constituents in the Zn-S catalyst contributed to the increase in O_3 decomposition and improvement of reaction rate with H_2O_2. Subsequently, the degradation of DB22 by the ozonation process with Zn-S catalyst was enhanced through the enrichment mechanism of hydroxyl radicals (*OH) and surface adsorption. The degradation mechanism of DB22 by hydroxyl radicals was surely affirmed by tests with the decrease in degradation percentage of DB22 in case of the presence t-butanol, Cl^- and CO_3^{2-}.

1. Introduction

Synthetic dyes are classified into different groups such as azo dyes, anthraquinone dyes, triarylmethine dyes, phtalocyanine dyes, etc. [1]. The most popular synthetic dyes discharged from textile wastewater are reactive azo dyes [2]. Besides, azo dyes are also widely used as an additive in other industries, for example plastic, leather, and paper industries [3]. Direct Black 22 (DB22) is one of popular anionic azo dyes used in dyeing cellulosic fibers like cotton, wool, viscose, rayon and paper. The presence of a high concentration of residual DB22 in wastewater can damage the environment due to its carcinogenicity, toxicity, recalcitrance, organic content and strong color. Therefore, their toxicity and recalcitrance to degradation pose a huge challenge towards removal technologies [3]. In order to combat this menace of pollution problem, it is desirable to degrade the dye into harmless form before its discharge into aquatic environment. DB22 contains azo

* Corresponding author.
E-mail addresses: nguyenthihien@tdtu.edu.vn (N.T. Hien), lanhuongba@gmail.com (L.H. Nguyen), tapvh@tnus.edu.vn (H.T. Van), dongnt@tnus.edu.vn (T.D. Nguyen), viennth@tnus.edu.vn (T.H.V. Nguyen), huyencth@tnus.edu.vn (T.H.H. Chu), tien.Nguyen@uts.edu.au (T.V. Nguyen), trvtuyen@ietvn.vn (V.T. Trinh), vuxuanhoa@duytan.edu.vn (X.H. Vu), kosar.hamaaziz@univsul.edu.iq (K.H.H. Aziz).

https://doi.org/10.1016/j.seppur.2019.115961
Received 2 July 2019; Received in revised form 7 August 2019; Accepted 19 August 2019
Available online 19 August 2019

linkages -N=N- bond, linking phenyl and naphthyl radicals (amino (-NH_2), chloro (-Cl), hydroxyl (-OH), methyl (-CH_3), nitro (-NO_2) and sulfonic acid sodium salt (-SO_3Na), which make DB22 stable and difficult to remove [1]. Provided conventional wastewater treatment systems such as traditional physical, chemical, and biological treatment methods are not able to degrade and remove recalcitrant organic pollutants, which are usually present in dyeing wastewater at high concentration level.

Various approaches and techniques have been applied to decolorize and decompose dyes, such as coagulation [4], adsorption [5,6], biological treatment [7–10], filtration [11], electrochemical [12], Fenton oxidation process [13,14] and photocatalytic methods [15], etc. However, these methods pose their specifically disadvantages or limitations, including low mineralization efficiency, high energy consumption, difficulty in handling large amounts of chemicals, sludge disposal, unsuitability to toxic compounds, requirement of a large area and higher residence time [16].

Currently, scientific and research community have shown their great interest in the treatment of textile industry dyes with so-called advanced oxidation processes (AOPs) which are widely applied to remove organic compounds from wastewater [17]. AOPs offer an extremely reactive and non-selective oxidant specifically hydroxyl radicals, capable of destroying a wide range of organic pollutants in wastewater. AOPs can be operated at ambient temperature and pressure, and subsequently, it can completely and non-selectively decompose and mineralize organic dyes to carbon dioxide, water and inorganic acids [18]. Amongst the oxidants used so far, ozone is considered to be one of the most powerful and favorable oxidants in eliminating toxic organic compounds. This is due to the good ability of ozone in oxidizing unsaturated double bonds and aromatic structures [16]. However, one of the main drawbacks of ozone application is the rate of slow reaction of ozone with some non-biodegradable organic compounds such as inactivated aromatics. Thus, to overcome this problem, catalytic ozonation processes have introduced to enhance oxidation of non-biodegradable organic compounds through the generation of hydroxyl radicals (*OH) which have higher oxidation potential than that of ozone alone. Many metal catalysts including Fe(II), Fe(III), Mn(II), Zn(II), Co(II), Ni(II), Cu(II), Ag(II) and Ti(II), etc., were used as homogenous catalysts for ozonation of organic compounds from water and wastewater [4]. Apart from this, heterogeneous catalysts such as TiO_2/Al_2O_3 [19,20], MgO nanocrystals [21], Fe/MgO [22], Ni/AC (activated carbon) [23], etc., were also used for ozonation.

However, almost heterogeneous catalysts for the ozonation process are synthesized by chemical or physical methods which are generally very expensive. Therefore, production and application of low cost catalysts for the ozonation process is necessary to reduce the treatment cost and increase the feasible application of AOPs. Among low cost catalysts, metal slags are emerging as an excellent catalyst due to their availability and low cost. In particular, metal slag wastes are discharged from mining activities. Many studies have used the wastes-treat-wastes technology as catalytic ozonation for removal pollutants from wastewater such as activated petroleum waste sludge biochar [24] and activated spent FCC catalyst [25]. In Vietnam, a huge amount of metal slag wastes (about 250,000 ton/year) is being released into the environment from ferrous and non-ferrous metallurgy processes. Solid waste from the conventional ferrous and non-ferrous metallurgy processes, including iron, copper, cadmium, lead and zinc slags can be utilized as catalysts in heterogeneous ozonation of azo dye. The use of these slags as low cost catalysts for ozonation of azo dye can remarkably reduce the cost of wastewater treatment and improve the reuse of solid waste. Hitherto, the studies about utilization metal waste slags to produce adsorbents and catalysts applied in environmental treatment have been quite scare. Thus, novelty of this study in utilization of solid waste to produce catalyst will contribute both removal of various persistent organic compounds from wastewater and reduce the cost of hazardous solid waste management, and bring the huge environmental and economic significances.

The aim of the present work, thus, was to choose the most suitable low cost catalyst from metal slags discharged from ferrous and non-ferrous metallurgy processes in Vietnam for ozonation of DB22 from aqueous solution. To achieve this purpose, five kinds of metal slag, including iron slag (Fe-S), copper slag (Cu-S), cadmium (Cd-S), lead slag (Pb-S) and zinc slag (Zn-S) were collected and tested their characteristics as well as mineralization and decolorization capacity of DB22 as the potential catalysts. Based on the initial laboratory results, the zinc slag (Zn-S) was selected and evaluated in a detailed study for its performance in removal of DB22. Here, the pH value and COD concentrations of aqueous solution were varied to identify the best catalytic performance. The mechanism concerning the heterogeneous ozonation process for decolorization and mineralization of DB22 was also identified.

2. Materials and methods

2.1. Materials and chemicals

Direct Black 22 (DB22, $C_{44}H_{32}N_{13}Na_3O_{11}S_3$, molecular weight of 1083.97 g/mol) was provided by Ria Dyes & Chemicals Co. (commercial name Direct Fast Black VSF600) and was used without further purification. Dye solutions were made by dissolving a predetermined amount of DB22 in ultrapure water. Five metal slags (Cd-S; Fe-S; Pb-S; Cu-S and Zn-S) were collected from solid wastes discharged by Thai Nguyen Non Ferrous Metals Limited Company, Thai Nguyen province, Vietnam. All metal slags were dried at 105 °C for 48 h, crushed and sieved to a powder size of less than 0.25 mm before storage in sealed plastic containers. These powdered slags were then used as heterogeneous catalysts for ozonation of DB22 in all experiments.

2.2. Experimental set-up

The scheme of ozonation systems was presented in Fig. 1. The dye mineralization was performed in batch process. Ozone was generated by an ozone generator (NextOzone 20P, International Ozone Joint Stock Company, Vietnam). The maximum capacity and capacity of ozone inlet O_3 at a flow rate of 15 mL/min was 5.0 g/h and 3.038 g/h. The generator's oxygen source was a pure oxygen cylinder. The newly produced ozone was distributed into a 1.2 L tubular borosilicate glass reactor (h = 450 mm, ϕ_{in} = 60 mm) through a diffuser located at the bottom of the reactor. Each kind of metal slag was separately added into the reactor containing 500 mL DB22 with a desired concentration of 0.125–1.0 g/L and at various pH (3–11). The ozonation time was 5 min for each cycle which in total lasted 40 min. The excess ozone in the outlet gas was absorbed by 1500 mL of 2% KI solution packed in 2000 mL conical flasks. The perozone (O_3/H_2O_2) and catazone (O_3/

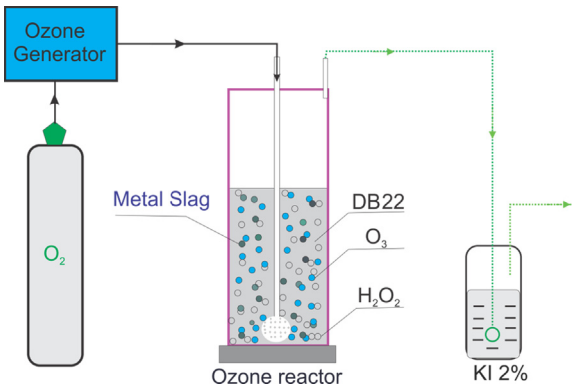

Fig. 1. General scheme of ozonation and perozone systems in DB22 mineralization.

H_2O_2/metal slags) reactions were carried out in duplicated systems. In the later reaction, H_2O_2 dosage of 100 mg/L was applied.

2.3. Analysis

The aqueous solution's color was measured by UV/Vis spectrophotometer (Shimadzu, model Z2000, Japan) at a wavelength of 481 nm while COD was determined according to standard method 5220 [26]. The solution pH was adjusted by using 0.1 M HCl and 0.1 M NaOH and was measured by a pH meter (HANNA, pH HI 2211-02, Romani). The ozone concentration in gas phase was measured using the iodometric wet – chemistry method [27]. The pH value of solution containing metal slags at the point of zero charge (pH_{PZC}) was determined by the Mular–Roberts titration technique [28].

The volume of pores and surface area of metal slags were determined by the Brunauer-Emmet-Teller method (BET) on SA 3000 (Coulter, USA). The surface morphologies of metal slags were observed by a scanning electron microscope (SEM) at 2.0 kV with different magnifications. The X-ray diffraction (XRD) pattern of metal slag particles was recorded using a Siemens D5005 X-ray diffract to meter with the CuKa radiation (λ = 1.5417 Å).

3. Results and discussion

3.1. Characteristics of metal slags

The physical properties of various metal slags are presented in Table 1.

The analysis results from Table 1 indicate that five kinds of metal slag can be categorized as a non-porous material because of low specific surface area (from 4.72 m^2/g for Cu-S to 18.33 m^2/g for Zn-S) and low pore volume (from 0.0346 cm^3/g for Cd-S to 0.0838 for Zn-S). Meanwhile, the pH_{PZC} values were between 2.54 (for Fe-S) and 6.57 (for Zn-S). Of the five metal slags, Zn-S has the highest specific surface area (18.38 m^2/g), total pore volume (0.0838 cm^3/g) and pH_{PZC} (6.47).

The SEM images of iron, copper, cadmium, lead and zinc slags are shown in Fig. 2. It can be observed from Fig. 2 that all metal slags have a non-uniform particle size. Furthermore, it emerged that some particles had a quasi-cubic shape.

Fig. 3 presents the EDS analysis of five metal slags. Fe-S analytical data confirms the presence of O, S, Si, Fe and Zn elements and the results of fraction ratios are presented in Fig. 3 with fraction ratios of 61.47%, 6.39%, 6.12%, 22.95% and 2.04%, respectively. Pb-S consists of O, Al, Si and Pb elements with amounts of 63.36%, 5.85%, 8.37% and 22.41%, respectively. There are three elements of O (69.90%), Ca (16.18%) and Zn (13.91%) in the zinc slag (Zn-S). Cd-S also consists of four elements, these being O (68.73%), S (10.34%), Cd (16.41%) and Zn (4.52%). The Cu-S component includes O (46.03%), S (22.52%) and Cu (31.44%).

The X-ray diffraction patterns of metal slags used as the catalyst for ozonation of DB22 are given in Fig. 4. It is evident that FeO, $Fe_3(SO_4)_2(OH)_6$, ZnO and SiO_2 exist in the Fe-S component. The presence of Cd, $CdCl_2(CH_5N_3S)).(H_2O)$ and ZnO was found in Cd-S. Pb-S contains $Pb(SO_4)$ and $KAl_2(Si, Al)_4O_{10}(OH)_2$. Cu, CuO and CuS_2 were present in the Cu-S. Zn-S consists of $CaCO_3$, $CaSO_4{\cdot}0.5H_2O$, $Zn(OH)_2$, and $CaSO_4{\cdot}2H_2O$ Most of the characteristic peaks were well indexed as amorphous with a highly graphite crystal structure in the XRD spectra of metal slags. This result was similar to the EDS data depicted in Fig. 3.

Table 1
Physical properties of metal slags.

Metal slag	S_{BET} (m^2/g)	Pore size (nm)	Pore volume (cm^3/g)	pH_{PZC}
Fe-S	7.99	25.44	0.0397	2.54
Zn-S	18.38	18.49	0.0838	6.57
Cd-S	7.24	12.88	0.0346	5.93
Cu-S	4.72	31.34	0.0370	5.44
Pb-S	16.75	24.54	0.0685	2.61

3.2. The DB22 removal efficiency of various metal slags

Initial experiments were carried out to compare the decolorization and mineralization of DB22 by heterogeneous catalytic ozonation with separately supplementation of Cd-S, Fe-S, Pb-S, Cu-S, Zn-S catalysts, ozone alone (O_3), and perozone (O_3/H_2O_2). The experiments were carried out using a metal slag dosage of 250 mg/L and solution pH values of 8.0 and the results are presented in Fig. 5. The ozone concentration was kept constant in the reactor by continuously adding ozone in bubble form. Results from Fig. 5 clearly indicate that the decolorization and mineralization efficiencies of DB22 differed when using heterogeneous catalysts produced from various metal slag wastes. In general, the treatment efficiency of DB22 by heterogeneous catalytic perozone (O_3/H_2O_2, Cd-S/O_3/H_2O_2, Fe-S/O_3/H_2O_2, Pb-S/O_3/H_2O_2, Cu-S/O_3/H_2O_2 and Zn-S/O_3/H_2O_2) was better than that of heterogeneous catalytic ozone (Cd-S/O_3, Fe-S/O_3, Pb-S/O_3, Cu-SO_3 and Zn-S/O_3) and O_3 alone. The results indicated that the presence of H_2O_2 in all ozonation systems enhanced decolorization and mineralization of DB22. This was due to the presence H_2O_2 in treatment systems reacted with O_3 as following reaction:

$$H_2O_2 + O_3 \rightarrow 2{*}OH + 3O_2 \quad (1)$$

The appearance of *OH after happened reactions oxidized DB22 leading to an increase in DB22 removal efficiency. Many studies indicated that optimum ratio of H_2O_2 and O_3 was 0.5. However, this ratio also depends on presence of *OH scavagers (Cl^-; HCO_3^-). In this study, it is easy to find that all ozonation systems with H_2O_2 had higher efficiency of decolorization and mineralization of DB22 proving that dosage of used H_2O_2 was suitable and the enhancement reaction rate followed above mentioned mechanism.

In addition, the decolorization was higher than the COD removal rate in all ozonation systems. The color of DB22 virtually disappeared after a short oxidation time of 20 min with the support of heterogeneous catalytic ozonation. In the meantime, the COD removal rate reached its highest level after 25 and 30 min with the presence of heterogeneous catalytic ozone and heterogeneous catalytic perozone, respectively. Also, the COD removal rate when utilizing heterogeneous catalytic perozone was higher than that of heterogeneous catalytic ozone.

The removal of COD and decolorization of DB22 were highest in heterogeneous catalytic ozonation with Zn-S, and then decreased in the following order: Pb-S > Fe-S > Cu-S > Cd-S > O_3/H_2O_2 > O_3 alone. With an initial DB22 concentration of 100 mg/L, COD removal reached 82% after 25 min oxidation by Zn-S/O_3 while it was 91% after 30 min oxidation with Zn-S/O_3/H_2O_2. In contrast, only 52% and 55% of COD removal was observed in O_3 and O_3/H_2O_2 oxidation, respectively. The presence of metal slags as low-cost catalysts significantly improved DB22 mineralization in terms of COD reduction and decolorization. This trend agreed with the findings reported by Hassani et al. (2019), who employed a Ni-containing layered double hydroxide nano-catalyst to degrade an azo dye methyl orange by catalytic ozonation [29].

It can be seen from Fig. 3 (EDS analysis results) that the weight proportions of total metal elements in Fe-S (Fe and Zn), Pb-S (Al, Si and Pb), Zn-S (Zn and Ca), Cd-S (Cd and Zn) and Cu-S (Cu) were 31.15%, 36.58%, 30.09%, 20.93% and 31.44%, respectively. The weight proportion of all metal elements in Zn-S was lower than that of Pb-S, nearly equivalent to Fe-S and Cu-S and higher than that of Cd-S. However, the efficiency of Zn-S as the catalyst for ozonation (heterogeneous catalytic ozone and heterogeneous catalytic perozone) was the highest. This indicates that the weight proportion was not a key factor for determining efficiency of heterogeneous catalytic ozonation of DB22. The physical properties of metal slags noted in Table 1 demonstrate that Zn-S had the

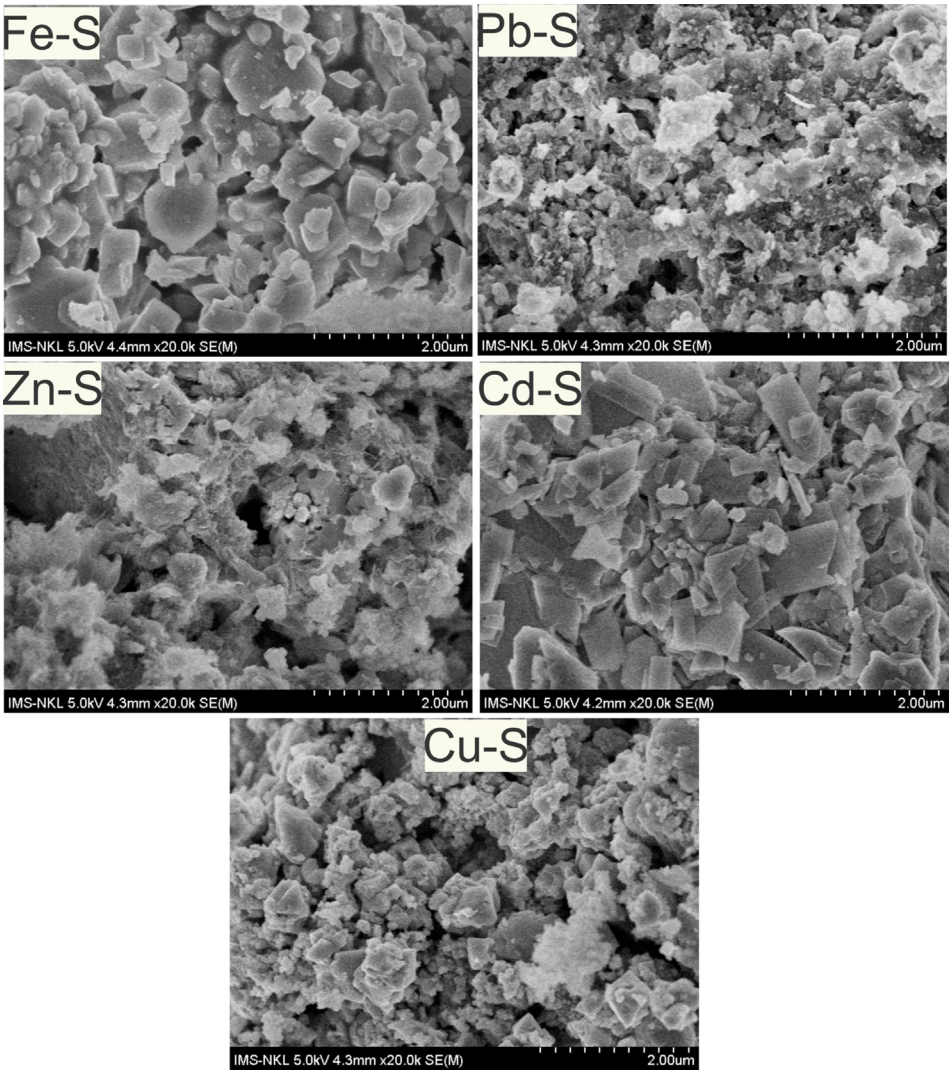

Fig. 2. SEM images of five kinds of metal slag (Cd-S, Fe-S, Pb-S, Cu-S, and Zn-S).

highest S_{BET} of 18.38 m^2/g, followed by Pb-S, Fe-S, Cd-S and Cu-S, respectively. Also the pore volume of Zn-S (0.0838 cm^3/g) was the highest. Therefore, it can be stated here that the pore volume and surface area were factors that strongly affected the decolorization and mineralization of DB22 in heterogeneous catalytic ozonation. The reason can be due to DB22 adsorbed onto Zn-S by pore filling mechanism.

The mineralization and decolorization increased when the catalyst surface and pore volume of each catalyst increased. This can be explained by the rising adsorption of O_3, H_2O_2 and DB22 on the catalysts [30]. Meanwhile, the pH_{pzc} of Zn-S was 6.57, higher than that of the other metal slags (Table 1). It indicates that the neutral surface of Zn-S was more active than other metal slags in promoting the generation of *OH radicals [31]. This led to the highest efficiencies of decolorization and mineralization of DB22, caused by an increase in contact and reaction on the Zn-S surface, specifically between O_3, H_2O_2 and metal elements of Zn-S (Ca and Zn). That increase enhanced the formation of hydroxyl radicals and subsequent oxidation of DB22 in both the solution and on the surface of Zn-S. The less developed oxidant types were generated by other ozonation systems when other metal slags were present. Consequently, the degradation rate of DB22 had the following order: Pb-S > Fe-S > Cu-S > Cd-S. These results also show that the heterogeneous catalytic ozonation system of DB22 was more efficient than O_3 alone.

Furthermore, these results agreed with several previous studies. In the report by Yildirim et al. (2011), the decolorization and mineralization efficiencies of Reactive Black 19 by O_3/Fe(II), O_3/Fe(II)/UVA, and O_3/TiO_2/UVA were higher than O_3 alone. A similar trend was also reported in a recent study on degradation of dimethyl phthalate by ozone alone and heterogeneous ozonation with Cu_xO-Fe_3O_4 nanoparticles [32]. El Hassani et al. (2019) also indicated that catalytic ozonation exhibited a faster reaction rate in decolorization and higher COD removal than that that of ozone alone. Therefore, the next experimental runs were conducted in the heterogeneous ozonation with only Zn-S as the catalyst, during which the highest degradation efficiency could be obtained.

3.3. The effect of pH on removal of DB22

The pH is an interesting parameter for the ozonation of water and wastewater. Heterogeneous catalytic ozonation of DB22 was studied at various initial pH levels of 3, 5, 7, 9 and 11. The results are shown in Figs. 6 and 7. The ozone concentration was also kept constant in the reactor. It can be seen that rates of decolorization and mineralization of DB22 at pH 11 were much faster than that at pH 9, 7, 5 and 3 in heterogeneous catalytic ozonation with Zn-S, ozone alone (O_3) and perozone (O_3/H_2O_2). With 30–35 min of reaction time and pH ranging from 3 to 11, COD removal efficiency reached 36–55%, 42–66%, 43–69% and 64–76% for O_3, O_3/H_2O_2, Zn-S/O_3 and Zn-S/O_3/H_2O_2, respectively. The DB22 mineralization rate reached its highest point at

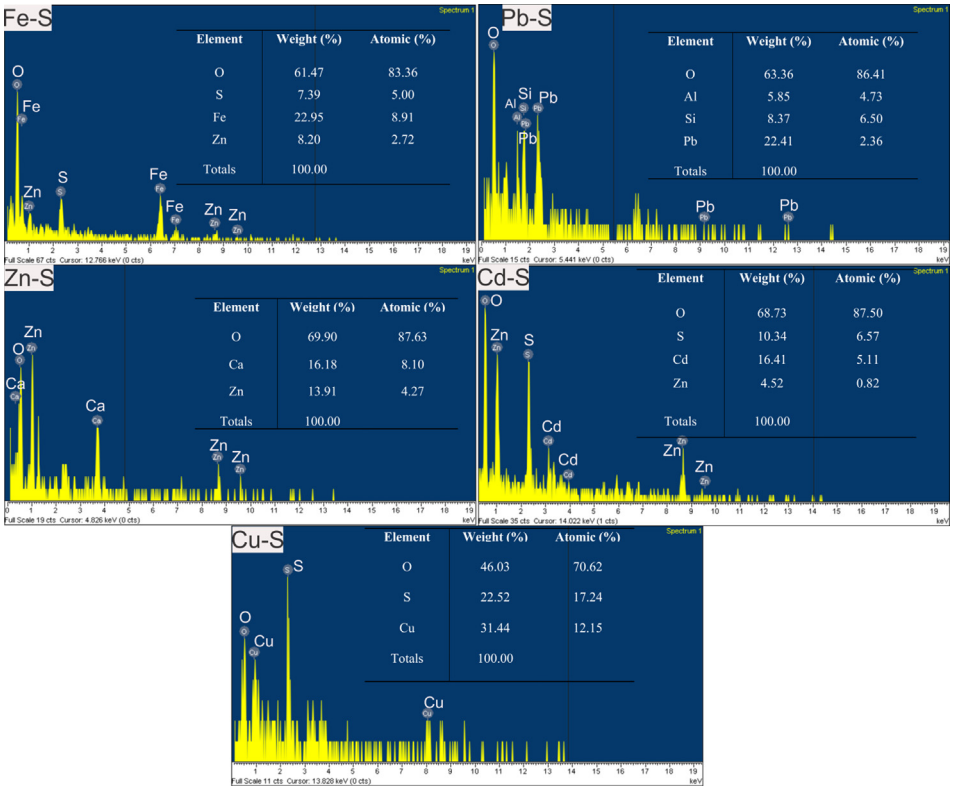

Fig. 3. EDS of five kinds of metal slag (Cd-S, Fe-S, Pb-S, Cu-S, and Zn-S).

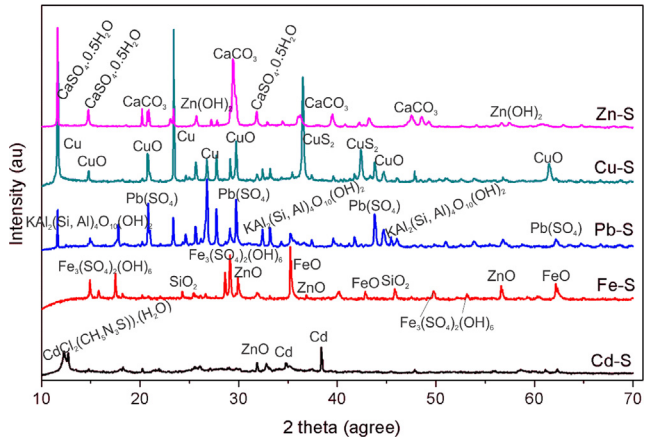

Fig. 4. XRDs graph of five kinds of metal slag (Cd-S, Fe-S, Pb-S, Cu-S, and Zn-S).

pH 11 and followed the order: Zn-S/O_3/H_2O_2 (after 30 min of reaction time: 76%) > Zn-S/O_3 (69%) > O_3/H_2O_2 (66%) > O_3 (55%). It means that pH plays an important role in enhancing the ozonation of DB22. Similar trends were observed by: Yildirim et al. (2011) investigated the removal efficiency of Reactive Red 194 by ozonation process at various pH from 3 to 11. The result indicated that optimum efficiency reached at pH of 11 [2]. The decolorization and mineralization of Reactive Blue 19 using ozonation process reached maximum at pH of 10 [33]. Similarly, in their study about heterogeneous catalytic ozonation in combination with natural clinoptilolite nanosheets to degrade nalidixic acid, Khataee et al. (2017) found that degradation efficiency of nalidixic acid increased in corresponding with an increase of pH from 3 to 9 [34].

In previous studies, Beltrán (2003) [35] and Moussavi et al. (2012) [36] reported that ozone can react with organic compounds in water and wastewater via a direct reaction pathway (attack by O_3 molecules at acidic pH) or an indirect way (attack via *OH radicals at alkaline pH), which considerably facilitated the reaction with the azo-groups, i.e. chromophore centers. Typically, at pH < 4, direct ozonation dominates and when pH ranges from 4 to 9, both are important, and at pH > 9 the indirect pathway dominates [38,39]. A direct electrophilic attack of the ozone molecule attracted at the acidic condition and undergoing selective electrophilic attack on the specific part of the organic compounds that have C=C bonds and/or aromatic ring to decompose them into carboxylic acid and aldehydes as the end products [40–42].

Ozone decomposition in water strongly depends on pH and occurs faster when the pH increases. The main oxidant species of organic compound produced by the ozonation process is molecular O_3 compared to *OH radicals at acidic conditions, which is due to the slower mineralization rate of ozone [31]. In a high pH medium, the ozone's oxidizing power increased remarkably due to the reaction between –OH in the solution with O_3, which resulted in the creation of superoxit O_2^- and hydroperoxit *OH_2. Here, O_3 continuously reacted with O_2^- to create *OH radicals. Therefore, direct ozonation is the dominant mechanism in acidic conditions. With this level of pH, the decolorization and mineralization rates of DB22 were the lowest using ozone alone (O_3) and both heterogeneous catalytic ozonation (Zn-S/O_3, Zn-S/O_3/H_2O_2) and heterogeneous catalytic perozone (O_3/H_2O_2). Meanwhile, ozone decomposition in water is strongly dependent on pH and occurs faster with an increase of pH. In addition, at pH > pH_{PZC}, the increase in aqueous ozone decay in the presence of natural materials could be related to ozone interaction with strong Lewis acid on metal oxides' surface sites [43]. In this study, the pH_{PZC} of Zn-S was 6.57. Thus, the ozone decay increased on the Zn-S surface in heterogeneous catalytic ozonation. Moreover, the catalyst accelerated the generation of hydroxyl *OH radicals derived from the catalysts' decomposition of ozone. This led to greater oxidation potential for enhancing the mineralization of organic pollutants [44]. Therefore, the decolorization and mineralization rates of DB22 through heterogeneous catalytic ozonation increased when pH increased, and were higher than that of ozone alone (O_3) and perozone (O_3/H_2O_2). This study also confirmed that maximum

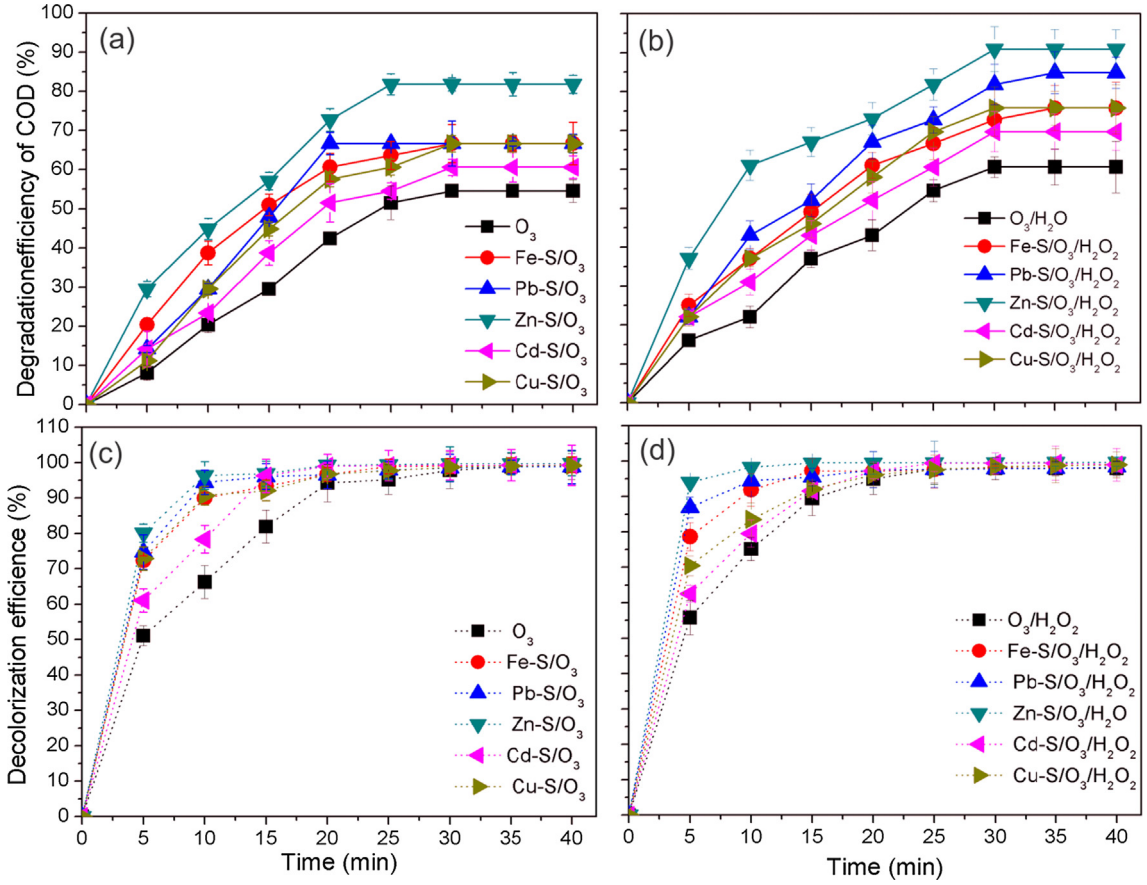

Fig. 5. Mineralization and decolorization of DB22 using various metal slags for (a and c) ozone alone and heterogeneous catalytic ozone and (b and d) heterogeneous catalytic perozone at 100 mg/L of COD; 3.038 g/h of inlet O_3, 100 mg/L of H_2O and 250 mg/L of catalyst dosage.

mineralization of DB22 by heterogeneous catalytic ozonation with Zn-S occurred at pH 11. Therefore, the next experiments were conducted at pH 11 in the heterogeneous ozonation with Zn-S as the catalyst.

3.4. The effects of metal slag (Zn-S) dosage

Fig. 8 present the effects of Zn-S dosage (0.125–1.0 g/L) on DB22 degradation through heterogeneous catalytic ozonation. The experiments were conducted at pH 11, the ozone generation rate of 3.038 g/h, initial H_2O_2 concentration of 100 mg/L, initial COD of DB22 of 100 mg/L for all treatment systems. It is observed that decolorization and minelization rates increased when elevating the Zn-S dosage from 0.125 g/L to 0.75 g/L for Zn-S/O_3 and from 0.125 g/L to 1.0 g/L for Zn-S/O_3/H_2O_2. However, these above rates fell when the dosage of Zn-S continued to increase from 0.75 to 1.0 g/L in the Zn-S/O_3 system. Thus, in terms of COD removal, the optimal Zn-S dosage was 0.75 g/L and 1.0 g/L in heterogeneous catalytic ozone (Zn-S/O_3) and heterogeneous catalytic perozone (Zn-S/O_3/H_2O_2), respectively. For the optimal Zn-S dosage, maximum COD removal efficiency after 25 min of reaction time was 67% and 74% for Zn-S/O_3 and Zn-S/O_3/H_2O_2, respectively. The decolorization rate was almost 99% in a shorter reaction time (10–15 min) in all heterogeneous catalytic ozonation of DB22. This result agreed with Hu et al. (2015), who reported that decolorization did not require too much catalyst in the reaction of catalytic ozonation of textile dyeing wastewater using mesoporous carbon aerogel supported copper oxide catalyst.

It is also found that DB22 dye's mineralization rate in the heterogeneous catalytic ozonation was higher than that in ozone alone and non-catalyst perozone. This was due to the increase in contact surface area and availability of reactive sites of catalyst for O_3, H_2O_2 and pollutants from aqueous solution [44,45]. This increased the reaction of O_3 and H_2O_2 (in Zn-S/O_3/H_2O_2) with metal elements which subsequently produced more *OH radicals. However, when the catalyst dosage exceeded the optimum amount, radicals were consumed by excess catalyst leading to a decline in degradation [4,39]. Here, the Zn-S may act as the inhibitor when Zn-S dosages of more than 0.75 g/L and 1.0 g/L were used in the Zn-S/O_3 and Zn-S/O_3/H_2O_2 system, respectively.

3.5. Kinetic and mechanism studies

The plot of Ln (C/C_o) versus reaction time was described by the following equation:

$$Ln\frac{C}{C_0} = -Kt \quad (1)$$

where C_0 and C are the concentrations of DB22 in aqueous solution at the beginning of reaction and at t min of reaction, respectively. When ln (C/C_0) was plotted versus time, the data fitted a straight line and the K (apparent first-order rate constant) value corresponded to the slope of the straight line.

Figs. S1–S3 show the values of K and regression coefficient (R^2) for the COD removal of DB22 in various metal slag catalysts, solution pH and metal slag dosage, respectively. The pseudo-first order kinetic model fits well with the experimental data (high values of regression coefficient ($R^2 > 0.95$)) for almost all ozonation processes involving DB22 mineralization. These findings accord with the discussion of the above DB22 mineralization, in terms of COD removal by heterogeneous catalytic ozonation regarding the effects of various metal slags, solution pH and Zn-S dosages. The obtained regression coefficients for the different investigated conditions show that mineralization of DB22 by heterogeneous catalytic ozonation with Zn-S followed the pseudo-first

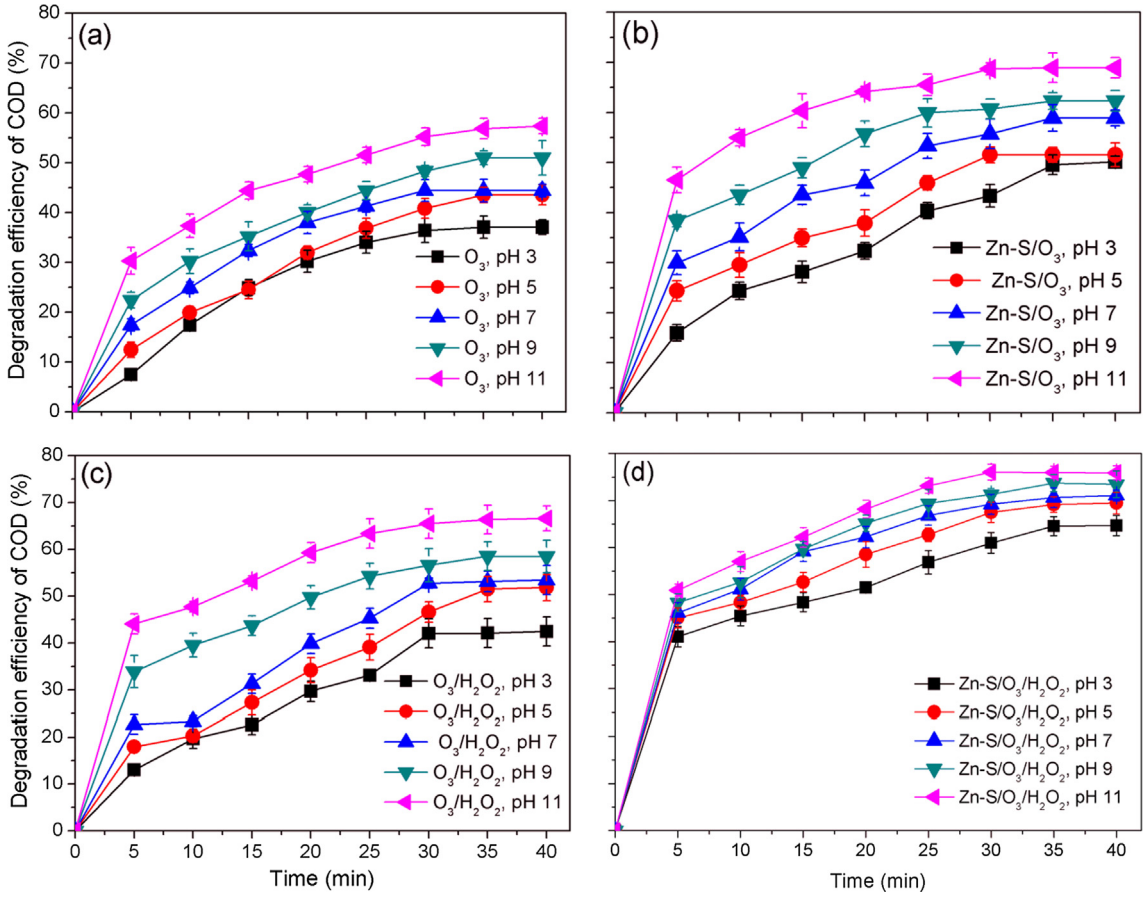

Fig. 6. Mineralization of DB22, in terms of COD removal, at various pH values for (a and b) heterogeneous catalytic ozone (O_3 and Zn-S/O_3); (c and d) heterogeneous catalytic perozone (O_3/H_2O_2 and Zn-S/O_3/H_2O_2) at 100 mg/L of COD; 3.038 g/h of inlet O_3, 100 mg/L of H_2O and 250 mg/L of catalyst dosage.

order kinetic and the apparent first-order rate constants were calculated from the slope of the plot.

When comparing different metal slag catalysts for ozonation of DB22, the K (min^{-1}) values decreased in the following order: Zn-S, Pb-S, Fe-S, Cu-S and Cd-S in both heterogeneous catalytic ozone and heterogeneous catalytic perozone. The calculated K values of DB22 under alkaline pH were higher than those under the neutral and acidic conditions (Fig. S2). In terms of the effect of Zn-S dosage on the pseudo-first order rate constant, K values were higher when increasing Zn-S dosage from 0.125 g/L to 0.75 g/L for Zn-S/O_3 and 0.125 g/L to 1.0 g/L for Zn-S/O_3/H_2O_2. However, K values decreased with a further increase in Zn-S dosage. Moreover, the K values of Zn-S/O_3/H_2O_2 were higher than that of Zn-S/O_3 in most cases.

Previous studies demonstrated that the reaction mechanism of ozonation process will be characterized by homogeneous and heterogeneous reactions: ozone self-decomposition reactions, and ozone decomposition promoted by metallic sites on the material surfaces [43]. Reactions on heterogeneous catalysts might involve several steps, for instance, ozone adsorption, ozone surface decomposition reactions, ozone decomposition reactions at the solid–liquid interface, and propagation reactions in the solution bulk [43]. Ca and Zn elements in the Zn-S can promote the decompostion of O_3 and H_2O_2 to produce more *OH radicals on the surface of Zn-S in Zn-S/O_3 and Zn-S/O_3/H_2O_2 systems, especially in alkaline conditions which improves decolonization and mineralization of DB22. The degradation mechanism of DB22 by heterogeneous catalytic ozonation might involve direct ozone self-decomposition reactions, adsorption, and generation mechanism of free radicals in solution and on the catalyst's surface.

Due to the existing components of $CaCO_3$, $CaSO_4{\cdot}0.5H_2O$, $Zn(OH)_2$, $CaSO_4{\cdot}2H_2O$ (see XRD data in Fig. 4) in Zn-S can act as both an adsorbent and heterogeneous catalyst. It can decompose O_3 in the Zn-S/O_3 system or react with H_2O_2 in the Zn-S/O_3/H_2O_2 system to improve the generation of *OH radicals. Through the electron transformation, some Zn and Ca elements in the Zn-S can be transformed to Zn^{2+}, Ca^{2+}. The latter can combine with ozone, leading to an improvement in the O_3 decomposition rate and production of hydroxyl radicals (*OH). There are three mechanisms: - H - atom abstraction, *OH addition to C═C, and *OH interaction with S, N atoms - that form *OH radicals in the heterogeneous catalytic ozonation of organic compounds [46,47]. Moreover, the removal mechanism of DB22 by Zn-S catalytic ozonation can be further clearly explained by the presence of Ca element in Zn-S constituent. DB22 is anionic dyes with sulfonate groups, which can form a complex with the calcium ions of $CaCO_3$ in Zn-S leading to a strong combination with the $CaCO_3$. Thus, $CaCO_3$ can adsorb DB22 efficiently and rapidly [48]. Additionally, the SEM image (Fig. 2) demonstrates that the morphology of the Zn-S with calcite materials is smooth cubic microcrystals. The adsorption of dyes by $CaCO_3$ materials could be attributed to the electrostatic interaction between Ca^{2+} and anionic organic dye molecules [49].

The next responsible mechanism for heterogeneous catalytic ozonation with the presence of Ca in catalyst's constituent was due to reaction between Zn with $CaCO_3$, $CaSO_4$ according to following reactions:

$$Zn + CaCO_3 \rightarrow ZnO + CaO + CO \quad (2)$$

$$Zn + CaSO_4 \rightarrow ZnSO_4 + Ca \quad (3)$$

Formed CaO on the catalyst's surface played role as an adsorbent; Meanwhile, ozone and generated *OH from ozone deposition became a oxidation agent, chelate with DB22. Ca-containing catalyst can react with O_3 and adsorb DB22. O_3 will oxidize Ca^{2+} to form hydroxyl

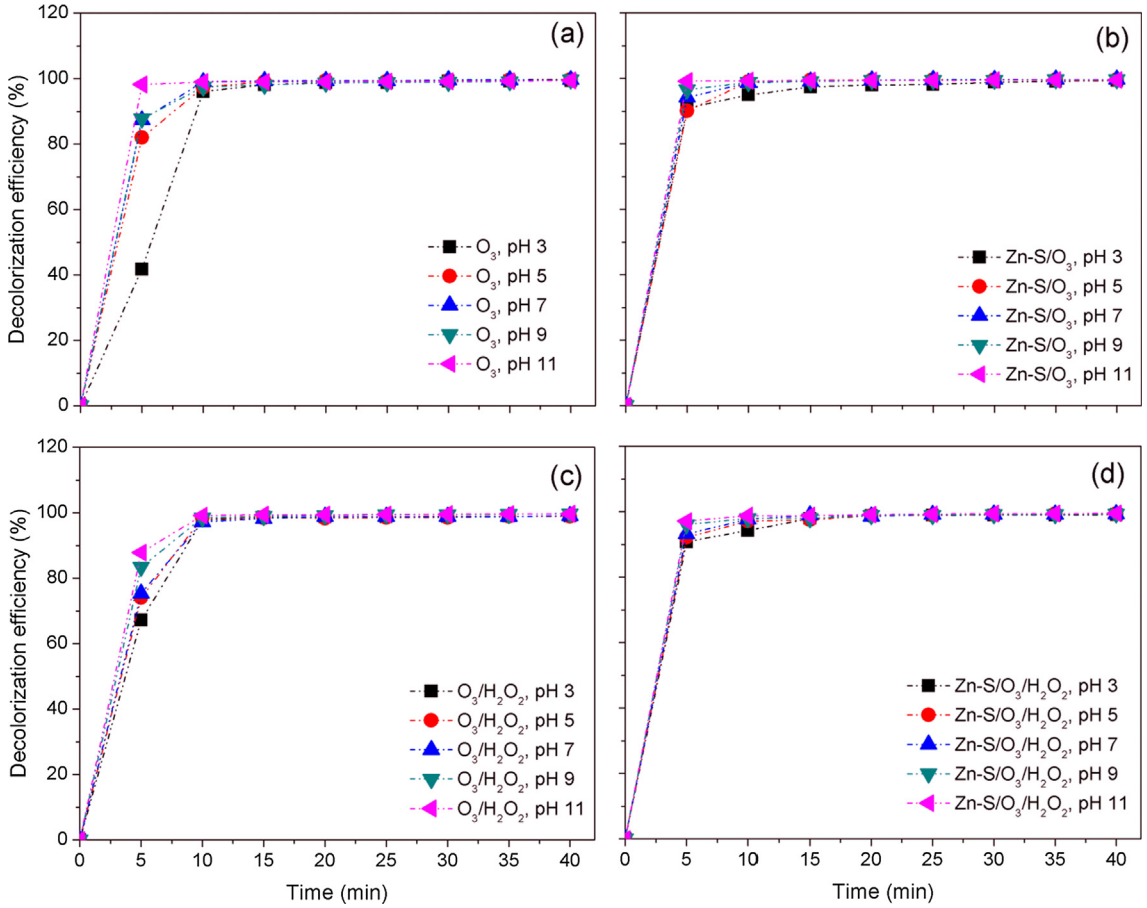

Fig. 7. Decolorization of DB22 at various pH values for (a and b) heterogeneous catalytic ozone (O_3 and Zn-S/O_3); (c and d) heterogeneous catalytic perozone (O_3/H_2O_2 and Zn-S/O_3/H_2O_2) at 100 mg/L of COD; 3.038 g/h of inlet O_3, 100 mg/L of H_2O and 250 mg/L of catalyst dosage.

radicals according to following reactions:

$$Ca + O_3 \rightarrow CaO + {}^*O_3 \quad (4)$$

$${}^*O_3 + H^+ \rightarrow {}^*HO_3 \quad (5)$$

$${}^*HO_3 \rightarrow {}^*OH + O_2 \quad (6)$$

DB22 was adsorbed on the oxidized metal catalyst and DB22 would be oxidized by the electronic transfer reaction, causing the catalyst to be reduced back to its original state and form the organic radicals adsorbed on the catalyst. The organic radicals were easily desorbed from catalyst and were continuously oxidized by *OH and O_3 in solution [50].

Thus, the presence of Zn and Ca elements in Zn-S played an important role in enhancing the generation of *OH radicals in Zn-S/O_3 and Zn-S/O_3/H_2O_2 for decolonization and mineralization of DB22.

The K values (apparent first-order rate constant) in heterogeneous Zn-S catalytic ozonation were higher than that of ozone alone and perozone. Also, the K values increased when increasing Zn-S dosages in heterogeneous catalytic ozonation of DB22. This may be attributed to the enhancement of generating hydroxyl radicals on the catalyst's surface, which initiated and promoted the degradation of azo dye [51]. These findings confirm the role of Zn-S in improving decolonization and mineralization of DB22 in ozonation systems.

In all above-mentioned treatment systems, the amount of *OH hydroxyl radicals increase with an increase in catalyst dosage. However, it is difficult to determine the concentration of hydroxyl radicals due to their short lifetime [46,52]. T-butanol, Cl^- and CO_3^{2-} have been used as popular and efficient hydroxyl radical scavengers to further verify degradation mechanism of DB22 by ozonation processes whether the attribution of hydroxyl radicals were or not. To conduct these experiments, various concentration of *t*-butanol, Cl^- and CO_3^{2-} were supplemented into treatment systems before the supplimentation of H_2O_2 and Zn-S. The obtained results are presented in Fig. 9.

The reaction rate constant of *OH with *t*-butanol is 6.2×10^8/$M^{-1}S^{-1}$ [34]. From Fig. 9, there was a decrease in the COD removal efficiency of all treatment systems with supplementation of *t*-butanol, Cl^- and CO_3^{2-}. This can be explained that the presence hydroxyl radical scavengers, namely, *t*-butanol, Cl^- and CO_3^{2-} in the ozonation systems of DB22 reacted with *OH leading to a consumption of *OH for reaction between *OH with these scavengers. Specially, at alkaline medium, more radical scavengers, such as CO_3^{2-}, SO_4^{2-} and Cl^- react favorably with *OH leading to a strongly decrease of the radical concentration [33]. At pH > 10, carbonate ions start to dominate in water and wastewater [53]. From Fig. 9, it can be seen that the degradation efficiency of DB22 decreased from to 49.10% to 42.79%, 36.44% and 16.73% for Zn-S/O_2; and from 57.49% to 51.54%, 48.32% and 22.27% for Zn-S/O_3/H_2O_2 in 40 min of reaction time when adding 100 mg/L of CO_3^{2-}, Cl^- and *t*-butanol, respectively. These results also demonstrated that *t*-butanol was the most strong hydroxyl radicals scavenger, followed by Cl^- and CO_3^{2-}. The decreased degradation efficiency with supplementation of CO_3^{2-}, Cl^- and *t*-butanol proved that *OH played a vital role in the degradation of DB22 in all heterogeneous catalytic ozonation systems in the presence of Zn-S.

In summary, from the experimental results and from referring similar researches, it is clear that in Zn-S heterogeneous catalytic ozonation, the presence of metal elements and hydrogen peroxide was the main factor determining the catalytic activity. The catalytic activity occurred mainly due to contribution of two mechanisms, namely, enhancement of *OH generation, and adsorption by complextion with

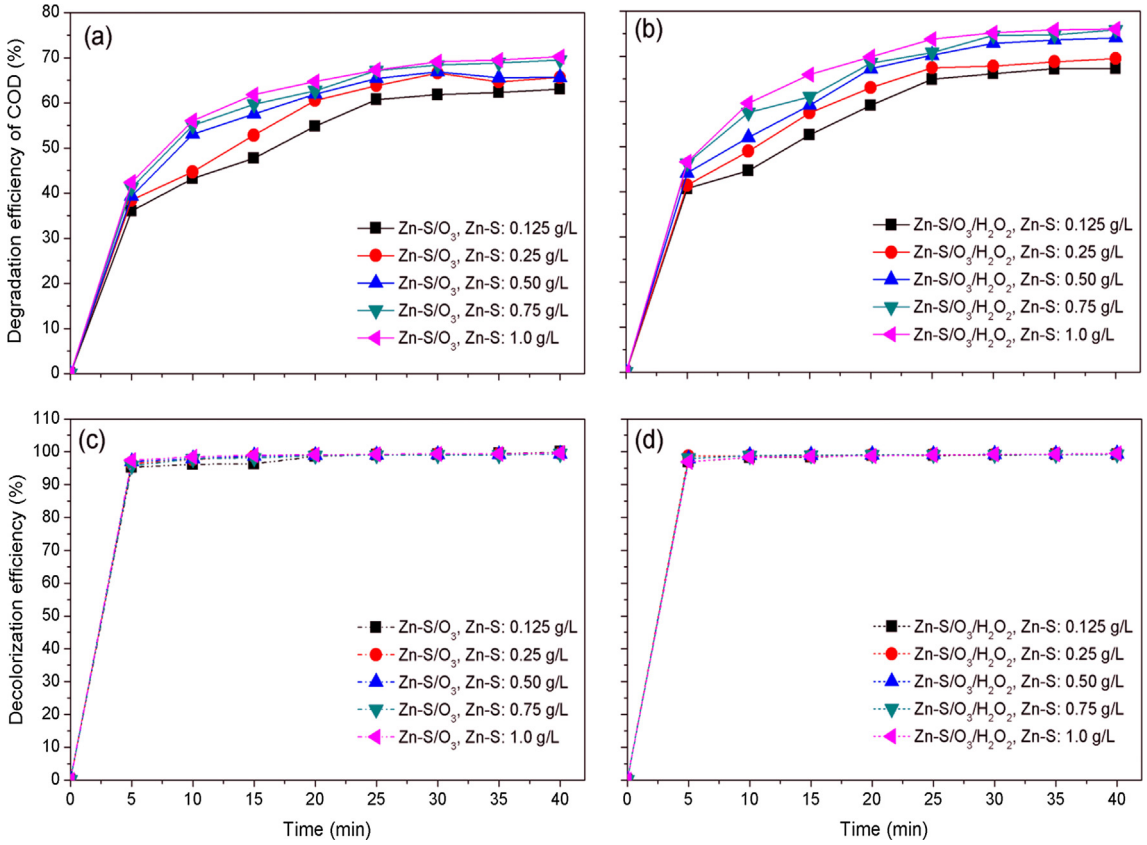

Fig. 8. Mineralization and decolorization of DB22 at various metal slag dosages for (a and c) heterogeneous catalytic ozone and (b and d) heterogeneous catalytic perozone at 100 mg/L of COD; 3.038 g/h of inlet O_3, 100 mg/L of H_2O and 250 mg/L of catalyst dosage.

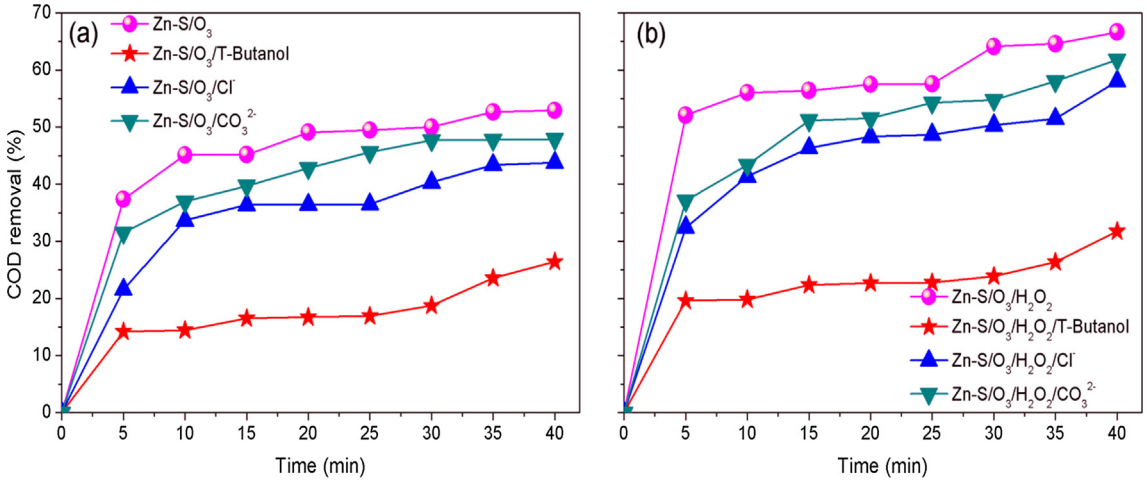

Fig. 9. Effect of t-butanol, chloride and carbonate on DB22 degradation, in term of COD removal by (a) Zn-S/O_3 and (b) Zn-S/O_3/H_2O_2 at 100 mg/L of COD, 3.038 g/h of inlet O_3, 100 mg/L of H_2O_2, 250 mg/L of Zn-S dosage, 100 mg/L of t-butanol, 100 mg/L of Cl^- and 100 mg/L of CO_3^{2-}.

organic pollutant, and electrostatic attraction.

4. Conclusions

In this study, zinc slag (Zn-S) emerged as a potential catalyst for heterogeneous catalytic ozonation to decolonize and mineralize DB22. The effect of solution pH on the decolorization and mineralization of DB22 followed the order: pH 11 > pH 9 > pH 7 > pH 5 > pH 3 for heterogeneous catalytic ozonation processes (O_3, O_3/H_2O_2, Zn-S/O_3 and Zn-S/O_3/H_2O_2). The decolorization and mineralization rate of DB22 increased when the Zn-S dosage rose from 0.125 g/L to 0.75 g/L for Zn-S/O_3 and 0.125 g/L to 1.0 g/L for Zn-S/O_3/H_2O_2. The decolorization rate of DB22 reached nearly 99% after 10 to 15 min reaction. However, the mineralization rate needed more time (25 min) to reach the maximum of 67% and 74% for Zn-S/O_3 and Zn-S/O_3/H_2O_2, respectively. The K values of the pseudo-first order model followed the same order as that concerning the mineralization rate (expressed in terms of COD removal) of DB22. The presence of Ca and Zn elements in Zn-S played an important role in decolorization and mineralization rate of DB22 when employing heterogeneous catalytic ozonation processes. Finally, the high decolorization and mineralization rate of azo dye may be attributed to the improvement in the generation of active radicals on

the Zn-S surface.

Acknowledgement

This research was funded by Vietnam National Foundation for Science and Technology Development (NAFOSTED), Vietnam, under grant number 105.99-2017.01.

Appendix A. Supplementary material

Supplementary data to this article can be found online at https://doi.org/10.1016/j.seppur.2019.115961.

References

[1] F. Gökçen, T.A. Özbelge, Enhancement of biodegradability by continuous ozonation in acid red-151 solutions and kinetic modeling, Chem. Eng. J. 114 (2005) 99–104, https://doi.org/10.1016/j.cej.2005.09.006.
[2] A.Ö. Yildirim, Ş. Gül, O. Eren, E. Kuşvuran, A comparative study of ozonation, homogeneous catalytic ozonation, and photocatalytic ozonation for C.I. reactive red 194 azo dye degradation, Clean - Soil, Air, Water. 39 (2011) 795–805, https://doi.org/10.1002/clen.201000192.
[3] F. Fahmi, C.Z.A. Abidin, N.R. Rahmat, Multi-stage ozonation and biological treatment for removal of azo dye industrial effluent, Int. J. Environ. Sci. Dev. 1 (2013) 193–198, https://doi.org/10.7763/ijesd.2010.v1.36.
[4] S. Khuntia, S.K. Majumder, P. Ghosh, Catalytic ozonation of dye in a microbubble system: hydroxyl radical contribution and effect of salt, J. Environ. Chem. Eng. 4 (2016) 2250–2258, https://doi.org/10.1016/j.jece.2016.04.005.
[5] H.T. Van, T.M.P. Nguyen, V.T. Thao, X.H. Vu, T.V. Nguyen, L.H. Nguyen, Applying activated carbon derived from coconut shell loaded by silver nanoparticles to remove methylene blue in aqueous solution, Water. Air. Soil Pollut. 229 (2018), https://doi.org/10.1007/s11270-018-4043-3.
[6] M. Kaykhaii, M. Sasani, S. Marghzari, Removal of dyes from the environment by adsorption process, Chem. Mater. Eng. 6 (2018) 31–35, https://doi.org/10.13189/cme.2018.060201.
[7] M.T. Yagub, T.K. Sen, S. Afroze, H.M. Ang, Dye and its removal from aqueous solution by adsorption: a review, Adv. Colloid Interface Sci. 209 (2014) 172–184, https://doi.org/10.1016/j.cis.2014.04.002.
[8] D. Bhatia, Neeta Raj Sharma, J. Singh, R. Kanwar, Biological methods for textile dye removal from wastewater: a review, Crit. Rev. Environ. Sci. Technol. (2017), https://doi.org/10.1080/10643389.2017.1393263.
[9] S.A.S. Chatha, M. Asgher, S. Ali, A.I. Hussain, Biological color stripping: a novel technology for removal of dye from cellulose fibers, Carbohydr. Polym. 87 (2012) 1476–1481, https://doi.org/10.1016/j.carbpol.2011.09.041.
[10] B. Abbasi, Removal of dye by biological methods using fungi, Int. J. Med. Rev. 4 (2018) 112–118, https://doi.org/10.29252/ijmr-040405.
[11] H.R. Rashidi, N.M.N. Sulaiman, N.A. Hashim, C.R.C. Hassan, M.R. Ramli, Synthetic reactive dye wastewater treatment by using nano-membrane filtration, Desalin. Water Treat. 55 (2015) 86–95, https://doi.org/10.1080/19443994.2014.912964.
[12] R. Salazar, M.S. Ureta-Zañartu, C. González-Vargas, C. do Nascimento Brito, C.A. Martinez-Huitle, Electrochemical degradation of industrial textile dye disperse yellow 3: role of electrocatalytic material and experimental conditions on the catalytic production of oxidants and oxidation pathway, Chemosphere 198 (2018) 21–29, https://doi.org/10.1016/j.chemosphere.2017.12.092.
[13] P.V. Nidheesh, R. Gandhimathi, S.T. Ramesh, Degradation of dyes from aqueous solution by Fenton processes: a review, Environ. Sci. Pollut. Res. 20 (2013) 2099–2132, https://doi.org/10.1007/s11356-012-1385-z.
[14] A. Tabaï, O. Bechiri, M. Abbessi, Degradation of organic dye using a new homogeneous Fenton-like system based on hydrogen peroxide and a recyclable Dawson-type heteropolyanion, Int. J. Ind. Chem. 8 (2017) 83–89, https://doi.org/10.1007/s40090-016-0104-x.
[15] S. Li, Q. Lin, X. Liu, L. Yang, J. Ding, F. Dong, Y. Li, M. Irfan, P. Zhang, Fast photocatalytic degradation of dyes using low-power laser-fabricated Cu_2O-Cu nanocomposites, RSC Adv. 8 (2018) 20277–20286, https://doi.org/10.1039/c8ra03117g.
[16] S.P. Ghuge, A.K. Saroha, Catalytic ozonation of dye industry effluent using mesoporous bimetallic Ru-Cu/SBA-15 catalyst, Process Saf. Environ. Prot. 118 (2018) 125–132, https://doi.org/10.1016/j.psep.2018.06.033.
[17] K.H. Hama Aziz, Application of different advanced oxidation processes for the removal of chloroacetic acids using a planar falling film reactor, Chemosphere 228 (2019) 377–383, https://doi.org/10.1016/j.chemosphere.2019.04.160.
[18] K.H. Hama Aziz, A. Mahyar, H. Miessner, S. Mueller, D. Kalass, D. Moeller, I. Khorshid, M.A.M. Rashid, Application of a planar falling film reactor for decomposition and mineralization of methylene blue in the aqueous media via ozonation, Fenton, photocatalysis and non-thermal plasma: s comparative study, Process Saf. Environ. Prot. 113 (2018) 319–329, https://doi.org/10.1016/j.psep.2017.11.005.
[19] F.J. Beltrán, F.J. Rivas, R. Montero-de-Espinosa, A TiO_2/Al_2O_3 catalyst to improve the ozonation of oxalic acid in water, Appl. Catal. B Environ. 47 (2004) 101–109, https://doi.org/10.1016/j.apcatb.2003.07.007.
[20] Y.H. Chen, D.C. Hsieh, N.C. Shang, Efficient mineralization of dimethyl phthalate by catalytic ozonation using TiO_2/Al_2O_3 catalyst, J. Hazard. Mater. 192 (2011) 1017–1025, https://doi.org/10.1016/j.jhazmat.2011.06.005.
[21] G. Moussavi, A. Khavanin, R. Alizadeh, The integration of ozonation catalyzed with MgO nanocrystals and the biodegradation for the removal of phenol from saline wastewater, Appl. Catal. B Environ. 97 (2010) 160–167, https://doi.org/10.1016/j.apcatb.2010.03.036.
[22] J.-E. Lee, B.-S. Jin, S.-H. Cho, S.-H. Han, O.-S. Joo, K.-D. Jung, Catalytic ozonation of humic acids with Fe/MgO, 2005. doi:10.1007/BF02706638.
[23] I. Ghouma, M. Guiza, M. Jeguirim, A.A. Zorpas, L. Limousy, A. Ouederni, An optimization study of nickel catalyst supported on activated carbon for the 2-nitrophenol catalytic ozonation, Desalin. Water Treat. 112 (2018) 242–249, https://doi.org/10.5004/dwt.2018.22303.
[24] C. Chen, X. Yan, Y.Y. Xu, B.A. Yoza, X. Wang, Y. Kou, H. Ye, Q. Wang, Q.X. Li, Activated petroleum waste sludge biochar for efficient catalytic ozonation of refinery wastewater, Sci. Total Environ. 651 (2019) 2631–2640, https://doi.org/10.1016/j.scitotenv.2018.10.131.
[25] C. Chen, J. Yu, B.A. Yoza, Q.X. Li, G. Wang, A novel “wastes-treat-wastes” technology: role and potential of spent fluid catalytic cracking catalyst assisted ozonation of petrochemical wastewater, J. Environ. Manage. 152 (2015) 58–65, https://doi.org/10.1016/j.jenvman.2015.01.022.
[26] APHA, Standard Methods for the Examination of Water and Wastewater Part 1000 Standard Methods for the Examination of Water and Wastewater, in: Am. Water Work. Assoc., 2012: pp. 1–541.
[27] K. Rakness, G. Gordon, B. Langlais, W. Masschelein, N. Matsumoto, Y. Richard, C.M. Robson, I. Somiya, Guideline for measurement of ozone concentration in the process gas from an ozone generator, Ozone Sci. Eng. 18 (1996) 209–229.
[28] M. Alvarez-Silva, A. Uribe-Salas, M. Mirnezami, J.A. Finch, The point of zero charge of phyllosilicate minerals using the Mular-Roberts titration technique, Miner. Eng. 23 (2010) 383–389, https://doi.org/10.1016/j.mineng.2009.11.013.
[29] K. El Hassani, D. Kalnina, M. Turks, B.H. Beakou, A. Anouar, Enhanced degradation of an azo dye by catalytic ozonation over Ni-containing layered double hydroxide nanocatalyst, Sep. Purif. Technol. 210 (2019) 764–774, https://doi.org/10.1016/j.seppur.2018.08.074.
[30] J.L. Rodríguez, I. Fuentes, C.M. Aguilar, M.A. Valenzuela, Catalytic ozonation as a promising technology for application in water treatment: advantages and constraints, IntechOpen (2018) 17–36.
[31] M.E. Lovato, C.A. Martín, A.E. Cassano, A reaction kinetic model for ozone decomposition in aqueous media valid for neutral and acidic pH, Chem. Eng. J. 146 (2009) 486–497, https://doi.org/10.1016/j.cej.2008.11.001.
[32] H. He, Y. Liu, D. Wu, X. Guan, Y. Zhang, Ozonation of dimethyl phthalate catalyzed by highly active CuxO-Fe_3O_4 nanoparticles prepared with zero-valent iron as the innovative precursor, Environ. Pollut. 227 (2017) 73–82, https://doi.org/10.1016/j.envpol.2017.04.065.
[33] M.E. Lovato, M.L. Fiasconaro, C.A. Martín, Degradation and toxicity depletion of RB19 anthraquinone dye in water by ozone-based technologies, Water Sci. Technol. 75 (2017) 813–822, https://doi.org/10.2166/wst.2016.501.
[34] A. Khataee, T.S. Rad, M. Fathinia, The role of clinoptilolite nanosheets in catalytic ozonation process: insights into the degradation mechanism, kinetics and the toxicity, J. Taiwan Inst. Chem. Eng. 77 (2017) 205–215, https://doi.org/10.1016/j.jtice.2017.05.004.
[35] F. Beltrán, Ozone Reaction Kinetics for Water and Wastewater Systems, Lewis Publishers Inc, New York, 2003. doi:https://doi.org/10.1201/9780203509173.
[36] G. Moussavi, R. Khosravi, N. Rashidnejad, Applied catalysis A: general development of an efficient catalyst from magnetite ore : characterization and catalytic potential in the ozonation of water toxic contaminants, Appl. Catal. A, Gen. 445–446 (2012) 42–49, https://doi.org/10.1016/j.apcata.2012.08.002.
[38] I. Arslan, I. Akmehmet, D.W. Bahnemann, Advanced oxidation of a reactive dyebath effluent : comparison of O3, H2O2/UV-C and TiO2/UV-A processes, Water Res. 36 (2002) 1143–1154.
[39] X. Zhang, W. Dong, W. Yang, Decolorization efficiency and kinetics of typical reactive azo dye RR2 in the homogeneous Fe (II) catalyzed ozonation process, Chem. Eng. J. 233 (2013) 14–23, https://doi.org/10.1016/j.cej.2013.07.098.
[40] K. Ikehata, M.G. El-Din, Degradation of recalcitrant surfactants in wastewater by ozonation and advanced oxidation processes: a review, Ozone Sci. Eng. 26 (2004) 327–343, https://doi.org/10.1080/01919510490482160.
[41] U. von Gunten, Ozonation of drinking water: part I. Oxidation kinetics and product formation, Water Res. 37 (2003) 1443–1467, https://doi.org/10.1016/S0043-1354(02)00457-8.
[42] W. Li, Q. Zhou, T. Hua, Removal of organic matter from landfill leachate by advanced oxidation processes: a review, Int. J. Chem. Eng. 2010 (2010) 1–10, https://doi.org/10.1155/2010/270532.
[43] H. Valdés, V.J. Farfán, J.A. Manoli, C.A. Zaror, Catalytic ozone aqueous decomposition promoted by natural zeolite and volcanic sand, J. Hazard. Mater. 165 (2009) 915–922, https://doi.org/10.1016/j.jhazmat.2008.10.093.
[44] E. Hu, W. Xinbo, S. Shang, X. Tao, S. Jiang, Catalytic ozonation of simulated textile dyeing wastewater using mesoporous carbon aerogel supported copper oxide catalyst, J. Clean. Prod. 112 (2015) 4710–4718, https://doi.org/10.1016/j.jclepro.2015.06.127.
[45] Y.D. Shahamat, M. Farzadkia, S. Nasseri, A.H. Mahvi, M. Gholami, A. Esrafili, Magnetic heterogeneous catalytic ozonation : a new removal method for phenol in industrial wastewater, J. Environ. HealSci. Technol. (2014) 1–12.
[46] H. Tap Van, L. Huong Nguyen, T. Kien Hoang, T. Pha Tran, A. Tuan Vo, T.T. Pham, X.C. Nguyen, Using FeO-constituted iron slag wastes as heterogeneous catalyst for fenton and ozonation processes to degrade reactive red 24 from aqueous solution, Sep. Purif. Technol. (2019), https://doi.org/10.1016/j.seppur.2019.05.048.
[47] X. Zhong, C. Cui, S. Yu, Exploring the pathways of aromatic carboxylic acids in

ozone solutions, RSC Adv. 7 (2017) 34339–34347, https://doi.org/10.1039/c7ra03039h.
[48] Z. Mengen, C. Zhenhua, L. Xinyan, K. Zhou, Z. Jie, T. Xiaohan, R. Xiuli, M. Xifan, Preparation of core – shell structured $CaCO_3$ microspheres as rapid and recyclable adsorbent for anionic dyes, R. Soc. Open Sci. 4 (2017) 170697, https://doi.org/10.1098/rsos.170697.
[49] K.Y. Chong, C.H. Chia, S. Zakaria, M.S. Sajab, Vaterite calcium carbonate for the adsorption of Congo red from aqueous solutions, J. Environ. Chem. Eng. 2 (2014) 2156–2161, https://doi.org/10.1016/j.jece.2014.09.017.
[50] B. Legube, N. Karpel, Vel Leitner, Catalytic ozonation: a promising advanced oxidation technology for water treatment, Catal. Today 53 (1999) 61–72, https://doi.org/10.1016/S0920-5861(99)00103-0.
[51] A. Manivel, G.J. Lee, C.Y. Chen, J.H. Chen, S.H. Ma, T.L. Horng, J.J. Wu, Synthesis of MoO_3 nanoparticles for azo dye degradation by catalytic ozonation, Mater. Res. Bull. 62 (2015) 184–191, https://doi.org/10.1016/j.materresbull.2014.11.016.
[52] J. Wang, Z. Bai, Fe-based catalysts for heterogeneous catalytic ozonation of emerging contaminants in water and wastewater, Chem. Eng. J. 312 (2017) 79–98, https://doi.org/10.1016/j.cej.2016.11.118.
[53] T.A. Ozbelge, F. Erol, Effects of pH, initiator, scavenger, and surfactant on the ozonation mechanism of an azo dye (acid red-151) in a batch reactor, Chem. Eng. Commun. 196 (2009) 39–55, https://doi.org/10.1080/00986440802303301.